Direct correlation of structure changes and thermal events in hydrated lipid established by simultaneous calorimetry and time-resolved x-ray diffraction

Hesson Chung and Martin Caffrey
Department of Chemistry, The Ohio State University, Columbus, Ohio 43210 USA

ABSTRACT In many lipid systems, polymorphic and mesomorphic behavior depends on sample thermal history. To establish unequivocally the structural origin of endothermic and exothermic events in such systems, we have performed simultaneous calorimetry and time-resolved x-ray diffraction (SCALTRD). To this end, aluminum calorimetry crucibles were used to contain the hydrated lipid sample, and the calorimeter was mounted with the base of the crucible oriented perpendicular to a synchrotron-derived focused monochromatic x-ray beam for SCALTRD data collection. Measurements were made with hydrated monoelaidin and 1,2-dielaidoyl-*sn*-glycero-3-phosphoethanolamine (DEPE) contained in hermetically sealed crucibles. Time-resolved x-ray diffraction (TRXRD) data were collected using an x-ray image intensifier/video system and a streak camera containing an x-ray sensitive image plate and/or film. SCALTRD analysis of the lamellar gel to lamellar liquid crystalline phase transition in hydrated monoelaidin gives identical progress curves by calorimetry and TRXRD at a scan rate of 1°C/min. At faster rates, calorimetry shows a broader phase transition that starts at a lower and ends at a higher temperature than is observed by TRXRD. The disparity arises in part because the x-ray beam used in TRXRD interrogates only a small portion of the sample, whereas the calorimeter responds to the entire sample volume. Because data collection times are relatively long, radiation damage is an important potential problem for SCALTRD measurements. Such an effect was observed with DEPE/water in that TRXRD shows the lamellar gel to lamellar liquid crystalline phase transition occurring at a lower temperature than observed by calorimetry. We speculate that the sample accumulates impurities locally as a result of radiation damage that has the effect of lowering the phase transition temperature at the site of interrogation by the x-ray beam. This "methods-in-combination" SCALTRD approach facilitates the direct correlation of structure rearrangements and thermal events in the same sample under identical conditions of thermal history. The information content of the data so derived far surpasses that available from either method used in isolation.

INTRODUCTION

An important aspect of lipid function in a variety of settings derives from the liquid crystalline character of lipids. Phase transitions between the various liquid crystalline states have been the focus of much attention for several decades, and a variety of methods have been used to study their thermodynamic, structural, and kinetic properties. Among them, calorimetry and x-ray diffraction have proven to be the most frequently used (Luzzati, 1968; McElhaney, 1986; Small, 1986). Calorimetry provides direct thermodynamic information, such as transition temperature and enthalpy change. Unfortunately, however, this method does not reveal the identity of the transforming phases. X-ray diffraction, on the other hand, is a method of choice for phase identification and structure characterization. With the advent of synchrotron radiation and the development of the time-resolved x-ray diffraction (TRXRD)[1] technique, it has been possible to use x-ray diffraction as a means for studying the kinetics and mechanism of phase transitions (see Caffrey, 1989, and references therein).

As such, the two methods, calorimetry and x-ray diffraction, neatly complement one another. A problem arises, however, in that in many lipid and lipid/water systems polymorphic and mesomorphic behavior can depend markedly on sample thermal history (Garti and Sato, 1988; Slater et al., 1989). Frequently, a number of thermal cycles are necessary before reproducible results are obtained. It is not uncommon to find in the literature that the first calorimetric scan has been omitted because of this effect. Metastability is another intriguing aspect of lipid mesomorphism (Caffrey, 1987; Seddon et al., 1983) that creates problems when data collected on samples with different thermal histories are compared. Method of sample preparation as well as the commercial source of the lipid can give rise to differences in mesomorphism (Finegold et al., 1985), which complicates comparisons of data collected using different methods under nonidentical conditions. These limitations can be overcome by performing calorimetry and TRXRD measurements simultaneously on the same sample. That such measurements in combination might be possible in hydrated lipid systems was suggested by simultaneous in-sample temperature and TRXRD measurements made on a fully hydrated phospholipid (Caffrey, 1985). In this study, a thermal halt was observed while the sample underwent a chain order/disorder transition monitored simultaneously by TRXRD. Concurrently, Russell and Koberstein (1985) reported simultaneous TRXRD and calorimetry on polymers using a method that has been implemented subsequently in other systems (Ungar and Feijoo, 1990; Kellens et al., 1991*a*, *b*). In the latter, simul-

[1] *Abbreviations used in this paper:* CHESS, Cornell High Energy Synchrotron Source; DEPE, 1,2-dielaidoyl-*sn*-glycero-3-phosphoethanolamine; I-2θ, intensity versus scattering angle; L_α, lamellar liquid crystalline phase; L_β, lamellar gel phase; NSLS, National Synchrotron Light Source; SCALTRD, simultaneous calorimetry and time-resolved x-ray diffraction (TRXRD).

0006-3495/92/08/438/10 $2.00

taneous measurements were relatively straightforward because sample hydration was not an issue. Indeed, in some of these studies, open calorimetry crucibles were used. Our focus is on hydrated lipid systems. In this communication, we describe a means for performing simultaneous calorimetry and TRXRD (SCALTRD) on such samples. The systems chosen for study include hydrated monoelaidin and hydrated 1,2-dielaidoyl-*sn*-glycero-3-phosphoethanolamine (DEPE), both of which undergo lamellar (L_β)-to-lamellar liquid crystal (L_α) phase transitions in an accessible temperature range. As a test of the performance of the SCALTRD method, measurements were made as a function of scan rate. It is shown that at lower scan rates the agreement between the two methods in SCALTRD measurements is remarkably good. In the case of DEPE, radiation damage proved to be a problem because the sample was exposed to a high flux x-ray beam for a prolonged period. Methods for minimizing radiation damage in SCALTRD measurements are described.

MATERIALS AND METHODS

Materials

Monoelaidin (Nu Chek Prep, Inc., Elysian, MN) and DEPE (Avanti Polar Lipids, Inc., Birmingham, AL) had a purity of ≥99% and ≥98%, respectively, as judged by thin-layer chromatography on silica gel K5F plates (Alltech Assoc., Inc., Deerfield, IL) of >100 μg lipid in three solvent systems (chloroform/methanol/water, 65:25:4 by vol; hexane/toluene/acetic acid, 60:40:1 by vol; chloroform/acetone/acetic acid/methanol, 72.5:25:0.5:2 by vol) and were used without further purification. At room temperature, monoelaidin consists of 90–92% 1-monoelaidin and 8–10% 2-monoelaidin (Martin, 1953). All other chemicals used were of reagent grade. Water was purified by using a water purification system (Milli-Q; Millipore Corp., Bedford, MA).

X-ray source

Measurements were made in the A1 and F1 stations at the Cornell High Energy Synchrotron Source (CHESS) and in the X12B station at the Brookhaven National Synchrotron Light Source (NSLS). In the A1 station at CHESS, experiments were carried out by using wiggler-enhanced monochromatic focused x-rays as previously described (Caffrey, 1985, 1987). X-ray wavelength (1.56 Å, 8.0 keV) was determined by using a lead nitrate standard and a carefully measured sample-to-film distance. The machine was operating at 5.26 GeV and 80 mA total of electron beam current in the seven-bunch mode and with the six-pole wiggler at half power. The incident x-ray beam was defined using a 0.5-mm-diameter collimator (Charles Supper Co., Inc., Natick, MA). Sample-to-detector distance was ~40 cm.

The F1 station at CHESS receives hard bend magnet as well as wiggler radiation from a 25-pole 1.2-T permanent magnet insertion device. This hybrid wiggler provides a beam with a critical energy of ~22 keV and has a peak field of 12 kG at the normal operating gap of 4 cm. Approximately 1–2 mrad of positron white synchrotron radiation passes through a 0.01-inch beryllium filter and two 0.015-inch water-cooled prefilters. The monochromator, located 20 m from the source, horizontally focuses and tunes the beam from 6 to 14 keV with one of two different bent asymmetrically cut Si (111) crystals miscut by 5.05°. A vertical focusing rhodium-coated Si mirror, the size of which is ~4 × 18 in, is available 0.8-m downstream of the monochromator. The focused beam has a 1.0-mrad horizontal and a 0.4-mrad vertical divergence. X-ray wavelength (13.6 keV, 0.92 Å) was determined by using a lead nitrate standard as above. The incident x-ray beam was defined using a 0.3-mm-diameter collimator (Supper Co., Inc.). Sample-to-detector distance was ~28 cm. Data were collected with Cornell Electron Storage Ring (CESR) operating at 5.26 GeV and 60 mA total of positron beam.

At NSLS, the x-ray beam was doubly focused by a 48-cm-long × 10-mm-wide 1:1 defocused rhodium-coated silicon carbide (primary) mirror and was passed through an 0.5-mm-diameter aperture block situated at the focal point of the primary mirror. The x-ray beam was monochromatized by a double fixed-exit silicon (111) flat crystal monochromator. The beam was doubly focused on the plane of the detector using a 1:1 defocused rhodium-coated electroless nickel-plated bent aluminum cylinder measuring 68 cm long and 3 cm wide. Before striking the sample, the beam was further defined by a set of slits and two sets of x-y guard slit arrays. X-ray wavelength (0.91 Å, 13.8 keV) at NSLS was determined by using a cholesterol myristate standard and a carefully measured sample-to-detector distance. The optical arrangement at NSLS enabled focusing of the beam to a point ~0.5 mm wide and 2 mm high at the detector. Sample-to-detector distances used at NSLS varied from 40 to 55 cm.

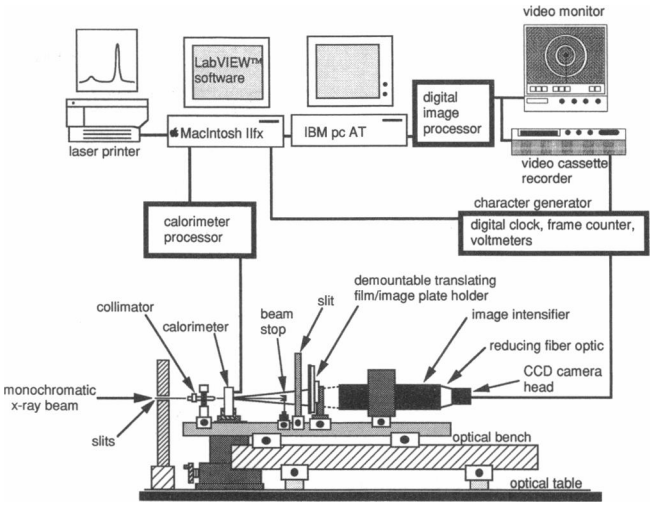

FIGURE 1 Schematic representation of the experimental arrangement for simultaneous calorimetry and TRXRD diffraction measurements at a synchrotron source. Focused monochromatic x-rays are collimated through a 0.5-mm-diameter collimator before striking the sample contained in an aluminum crucible within the calorimeter. Transmitted x-rays are intercepted by a remotely controlled nickel beam stop. When the streak camera is used for diffraction data collection, x-ray sensitive film and/or an image plate in a demountable holder is translated at a fixed rate behind a long narrow slit. When the image intensifier based system is used, the demountable film/plate holder is removed and the diffracted x-rays are allowed to strike the fluorescent screen of a three-stage intensifier tube used for image intensification. The image is displayed dynamically on the intensifier tube and recorded in live-time using a fiber optically coupled charge coupled device (CCD) camera and a super VHS video cassette recorder. Along with the two-dimensional diffracted image, the temperature, experiment number, and elapsed time in seconds and video frame number are recorded simultaneously on video tape. The operation of the calorimeter and the streak camera as well as data collection from the calorimeter are under computer control.

Simultaneous calorimetry and TRXRD

A calorimeter (model FP84; Mettler Instrument Corp., Hightstown, NJ), originally designed for simultaneous calorimetry and polarized light microscopy, was used in this application. Fig. 1 shows a schematic

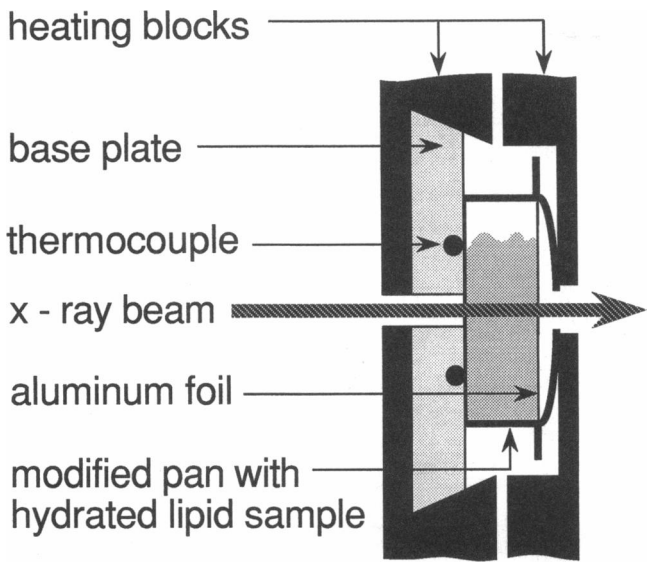

FIGURE 2 Schematic of the sample crucible arrangement in the calorimeter for simultaneous calorimetry and TRXRD. The sample and reference (not shown) pans are heated by contact with heating blocks that surround them. The temperature difference between the sample and reference is measured using five thermocouple sensors positioned on the base plate and in direct contact with the bottom of the pan. The sample crucible has been modified to increase x-ray transmittance as described in the text under Materials and Methods.

of the experimental arrangement for SCALTRD measurements at the synchrotron. The sample crucible in the calorimeter was mounted orthogonal to the incident x-ray beam on an optical bench (Fig. 2). The calorimeter was in turn mounted on a pair of translating stages for positioning of the sample pan in the x-ray beam. Fig. 2 shows how the sample pan has been modified for SCALTRD measurements and how it is positioned in the calorimeter. The FP84 includes two glass plates on either side of the sample pan that act as heat filters. In the SCALTRD application, these plates were removed to facilitate x-ray transmission with little if any effect on the performance of the device as a calorimeter. Temperatures below room temperature were achieved by supplying the calorimeter with cooled air from a forced-air crystal heating/cooling apparatus (models XR-85-1A-0 and AD-80XA; FTS Systems, Inc., Stone Ridge, NY).

Two types of detectors were used to record live-time x-ray diffraction patterns during SCALTRD. One of these detectors consists of an image intensifier/video-based system, and time-resolved diffraction patterns were recorded on S-VHS video tape (Panasonic, Japan) as described previously (Caffrey 1985, 1987; Caffrey et al., 1991*a*). The other is a streak camera that uses x-ray sensitive film (DEF5; Eastman Kodak Co., Rochester, NY) and/or image plates (storage phosphor, Eastman Kodak Co.) and that is translated at a rate of 4 mm/min behind a long vertical 3.2-mm-wide slit. Because a finite slit width is used, data collected with the streak camera have time and temperature resolution compromised somewhat in the present application. For example, with a 3.2-mm-wide slit and a film translating speed of 4 mm/min, each spatial element on the film or plate is exposed for $\leq$[3.2 mm/(4 mm/min)] = 0.8 min (48 s). With a temperature scan rate of 5°C/min, the corresponding temperature range that each spatial element samples is $\leq$[5°C/min $\times$ 0.8 min] = 4°C. The time resolution of the video tape was 33 ms.

Using the streak camera detector, both low- and wide-angle diffraction from the lipid sample was recorded simultaneously on the same film. With the image intensifier/video system, only the low-angle diffraction data were recorded. In the latter case, a character generator was used to insert elapsed time, experiment number, and temperature output from the calorimeter directly onto the video image during taping so that the three parameters are recorded simultaneously along with the two-dimensional diffraction pattern.

The calorimeter and the streak camera were operated under computer (Macintosh IIfx; Apple Computer, Inc., Cupertino, CA) control using LabVIEW™ (National Instruments, Austin, TX) software. A LabVIEW program was written to index simultaneously the calorimetry and streak film data with the beginning and end of an experiment. The same program was used to record and to display in real-time the thermogram on a MacIntosh IIfx; Apple Computer, Inc., Cupertino, CA computer as the experiment was performed. When the video system was used to record live diffraction patterns, the calorimeter and the video cassette recorder (S-VHS model 7500A; Panasonic, Japan) were not synchronized automatically. In this case, temporal alignment was made by using the temperature data that were recorded simultaneously on the computer and on the video image for calorimetry and TRXRD, respectively.

Sample crucibles

The aluminum cannisters (model 27331, Mettler Instrument Corp.) for use in the calorimeter were modified to increase their x-ray transmittance for SCALTRD measurements. The cannisters come in two parts: a pan and a lid. The bottom of the pan is ~0.2 mm thick and has an aluminum positioning pin (~0.8 mm long) at its center. The lid is 0.1 mm thick. Thus, an intact sealed pan has a total aluminum thickness of 1.1 mm along the flight path of the x-ray beam, which is sufficient to attenuate the x-ray beam to an unusable level at the available energies. X-ray transmittance is calculated as follows:

$$\frac{I}{I_0} = e^{-(\mu/\rho)\rho x}, \qquad (1)$$

where I and I_0 are the transmitted and the incident beam intensities, respectively, μ is the linear absorption coefficient, ρ is the density of the material, μ/ρ is the mass absorption coefficient, and χ is the thickness of the absorbing layer. The quantity μ/ρ is a characteristic of the absorbing material and varies with incident x-ray wavelength (Klug and Alexander, 1974). For aluminum, the μ/ρ value is ~49.4 at 1.55 Å and 10.2 at 0.90 Å and ρ is 2.70 g/cm^3 at 20°C (Macgillavry and Rieck, 1962). These values were used to calculate transmittance, assuming that the μ/ρ values above hold at 1.56 Å and at 0.91 Å. Using Eq. 1, the x-ray transmittance of the intact crucible at its center is 4.3×10^{-5} and 4.8% at 1.55 and 0.90 Å, respectively. By removing the positioning pin, reducing the thickness of the pan base from 0.2 to 0.1 mm, and replacing the lid with 10-μm-thick aluminum foil (Reynolds Metals Co., Richmond, VA), the total thickness of aluminum in the x-ray beam was reduced to 0.11 mm, corresponding to a transmittance of 23.1 and 73.9% at 1.55 and 0.90 Å, respectively. Such transmittance values for the modified crucibles mean that TRXRD measurements can be performed with relative ease given the x-ray flux and wavelengths available at CHESS and NSLS. To secure positioning of the cannister in the calorimeter, it was necessary to include the lid in the final assembly. However, a lid with a 1.5-mm-diameter hole in its center served the purpose and did not contribute to x-ray attenuation.

Sample preparation

Samples were prepared in excess water by placing ~10 mg of pure lipid and 25 μl of water in a modified aluminum pan. The top of the pan was covered with aluminum foil, and a lid with a hole in its center was placed on top of the foil and the entire assembly was press sealed (model 27339, Mettler Instrument Corp.). Extra foil around the outside of the pan was carefully removed, and the pan was finally sealed around the rim with a minimum amount of glue (SuperBonder; Loctite Co., Newington, CT).

Possible adverse effects of the glue were evaluated by calorimetry. When tested in the range 4–70°C, the glue was found to have no effect

on the shape or transition temperatures of lipid thermograms. Without modification, the press-sealed crucibles remain sealed up to 90°C. Beyond this temperature, we find consistently that the baseline of thermograms recorded on hydrated lipid samples increases, suggesting that the seal has broken and that water is evaporating and escaping from the crucible. The modifications we have effected on the crucibles gives reliable thermograms up to 70°C. However, above 70°C the cans begin to leak. Therefore, before performing SCALTRD measurements, each sample in a modified cannister is tested in the calorimeter to determine if it is leak-proof up to 70°C. Those that leak below 70°C are discarded. Our success rate is typically 70–80% in preparing modified cannisters useful to 70°C.

The internal volume of the modified crucible is 40 μl. To ensure that there is sample in the 0.5-mm-diameter x-ray beam as it passes through the center of the cannister, sample volumes of ≥25 μl are used.

Data analysis

The video-recorded data are quantified by digital image processing (Trapix 55/48; Recognition Concepts, Inc., Carson City, NV) using a combination of commercial (RTIPS; Tau Corp., Dayton, OH) and home-written software as described previously (Caffrey et al., 1990; Mencke and Caffrey, 1991). Sequential digitized images or parts thereof are "grabbed" and stored in the memory of the image processor. Intensity versus scattering angle (I-2θ) scans are made by averaging over a 20° arc centered on the vertical diameter. The data are then ported to a MacIntosh IIfx computer where they are processed further to resolve composite images into their components. The 001 diffraction peaks of the L_α and L_β phases were fitted by a nonlinear least-square method to the model function,

$$f_{\text{fit}}(x; M_\beta, \beta_\beta, \epsilon_\beta, M_\alpha, \beta_\alpha, \epsilon_\alpha, D) = M_\beta e^{-[(x-\beta_\beta)/\epsilon_\beta]^2} + M_\alpha e^{-[(x-\beta_\alpha)/\epsilon_\alpha]^2} + D, \quad (2)$$

where M is peak height, β is peak radial position, ϵ is peak half-width at half-height, D is a constant, and the subscripts α and β refer to the L_α and the L_β phases, respectively. Peak area, A, is calculated as

$$A = k\epsilon M, \quad (3)$$

where k is the proportionality constant $\pi^{1/2}$ (Caffrey et al., 1990; Mencke and Caffrey, 1991).

A static x-ray diffraction pattern of the L_β phase in hydrated monoelaidin at 10.1°C recorded with a known sample-to-film distance and periodicity (001 = 60.5 Å) was used to calibrate the two-dimensional video image.

Radiation damage

To minimize lipid radiation damage, a new portion of the sample was exposed for each SCALTRD measurement. Thus, no one part of the sample was exposed to the x-ray beam for >20 min. Experiments to test for radiation damage were carried out before SCALTRD measurements. We assume that damage is negligible if there is no detectable change in the diffraction pattern during a typical x-ray exposure when other variables, such as temperature, pressure, etc., are held constant. In the case of monoelaidin in water, a 2-h exposure at NSLS produced no noticeable change in the diffraction pattern at 38°C. However, on the A1 line at CHESS, damage to hydrated monoelaidin at 38°C was apparent after an exposure of 10 min. Damage was evidenced by the appearance of the so-called x-phase (Caffrey, 1987) in an L_α phase background. As a result, we consistently held exposures at single sites in the sample to ≤10 min at CHESS and ≤20 min at NSLS to minimize the damaging effects of x-rays. Radiation damage of DEPE is treated separately under RESULTS. A more complete analysis of radiation damage will be presented elsewhere (Cheng, A., and M. Caffrey, manuscript in preparation).

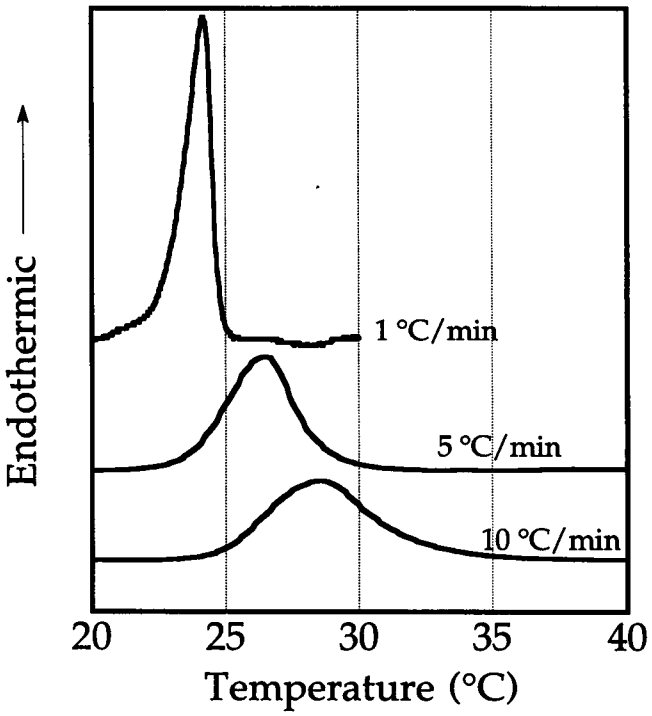

FIGURE 3 Heating thermograms of monoelaidin in excess water at the scan rates indicated. The sample consisted of 8–10 mg monoelaidin in 25 μl water.

RESULTS

Monoelaidin in water

The first set of SCALTRD measurements was made using monoelaidin in water with a focus on the L_β-to-L_α transition that occurs at ~23°C. Data were collected in the 10–40°C range, and the effect of scan rate from 1 to 10°C/min on the fidelity of the SCALTRD data was evaluated. The calorimetric results are shown in Fig. 3 for heating rates of 1, 5, and 10°C/min. The onset temperature of the order/disorder endotherm increases and the transition broadens as the heating rate increases. The onset temperatures, T_i, are 22.7, 23.5, and 24.9°C at heating rates of 1, 5, and 10°C/min, respectively. The corresponding transition widths (half-width at half-height) are 0.6, 1.5, and 2.3°C. The scan rate dependence of T_i and of the transition width suggests that the true values are less than those observed at 1°C/min because of the finite response time of the calorimeter.

Selected low-angle TRXRD images from the SCALTRD measurements recorded at 1°C/min are shown in Fig. 4. The original unprocessed two-dimensional low-angle diffraction images and how these change with temperature through the L_β-to-L_α phase transition at a heating rate of 1°C/min are presented in this figure. Included is the 001 lamellar reflection from the L_β phase (61 Å) at 22°C, the 001 lamellar reflection from the L_α phase (52 Å) at 28°C, and the two coexisting

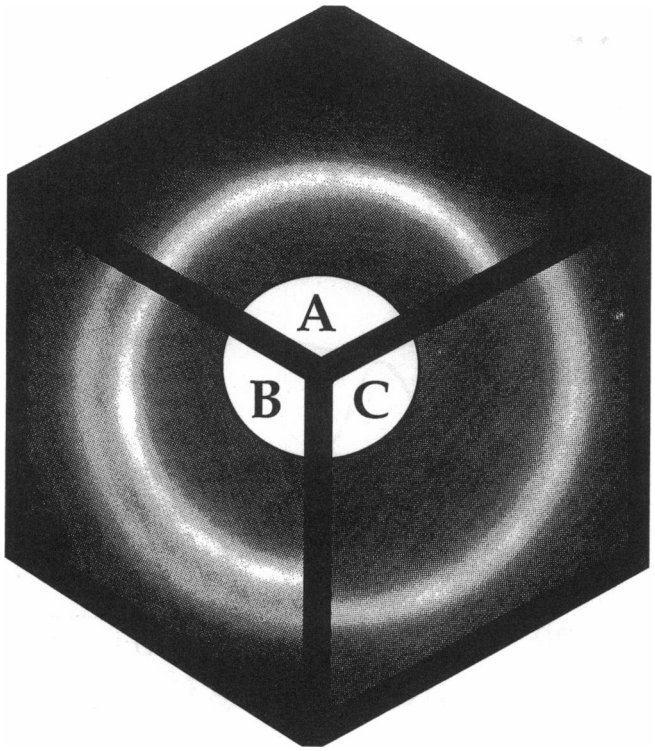

FIGURE 4 Progress of the L_β-to-L_α phase transition in fully hydrated monoelaidin monitored by TRXRD using an image intensifier/video-based detector system. Low-angle x-ray diffraction corresponding to the 001 reflection of the L_β and L_α phases were recorded continuously in live-time on video tape at the rate of 30 frames/s. Shown in this figure is a composite of three images representing the integration of 16 (0.53 s) enhanced video frames. Sectors *A* and *C* show the 001 lamellar reflections from the L_β and L_α phases at 22 and 28°C, respectively. Sector *B* shows coexistence of two 001 reflections: one from the L_β phase and one from the L_α phase recorded at 24°C midway through the transition. The heating rate used was 1°C/min.

L_β and L_α 001 reflections midway through the transition at 24°C.

The quantitative low-angle diffraction data obtained by image processing and how these change with temperature through the L_β-to-L_α phase transition of hydrated monoelaidin are presented in Fig. 5. As outlined under Data analysis, the diffraction data are fitted as a composite of 1 or 2 Gaussians and a constant. The parameters of each Gaussian, namely, peak position (β), height (M), and half-width at half-height (ϵ), along with the peak area (A), are shown as a function of temperature from 10 to 40°C in Fig. 5 *A–E* during a SCALTRD measurement made at 5°C/min. The corresponding calorimetric data (Fig. 5 *F*) shows onset and completion temperatures of 23.4 and 29.0°C, respectively, with a maximum heat capacity change at 26.5°C. By comparison, all of the parameters of the 001 diffraction peaks show a sharper transition with the bulk of the transition taking place in the interval 24.0–26.5°C. Therefore, at a heating rate of 5°C/min, the onset temperatures of the transition are in reasonable agreement by TRXRD and calorimetry. However, the completion temperature discrepancy is quite marked at this rate. The temperature range of the L_β-to-L_α transition determined by calorimetry and by TRXRD in SCALTRD measurements is presented as a function of heating rate in Fig. 6 *A*. At the slowest heating rate of 1°C/min, the two methods show essentially identical phase transition temperature ranges. At the higher scan rates of 5 and 10°C/min, the discrepancy between the two methods grows with the biggest difference observed in the completion temperature at the highest scan rate.

DEPE in water

In an effort to evaluate the versatility of the SCALTRD technique, measurements were also performed on fully hydrated DEPE in the temperature range 20–60°C. In this case, the L_β-to-L_α transition is centered at 38°C, some 14°C higher than the corresponding transition in monoelaidin. The SCALTRD results are summarized in Fig. 6 *B*, which shows the onset and completion temperature of the order/disorder transition recorded in the heating direction as a function of heating rate. As observed with monoelaidin, the transition determined by calorimetry is quite sharp at a scan rate of 1°C/min and broadens severalfold on increasing the scan rate to 10°C/min. The onset temperature is shifted to higher temperatures at the higher scan rates. Unlike the results observed with monoelaidin, however, at all heating rates used both the onset and completion of the transition occurred at a considerably lower temperature when measured by TRXRD. This result proved to be quite a mystery until it was demonstrated that the sample had succumbed to radiation damage in the course of the SCALTRD measurement. To test the radiation damage hypothesis, the following experiment was performed. Fully hydrated DEPE in an x-ray capillary at 35.4 ± 0.5°C was irradiated continuously with 13.8 keV x-rays while the diffraction from the sample was being recorded in the F1 station at CHESS. At the beginning of the exposure, the sample was in the L_β phase. However, within 5 min, the L_α phase emerged and continued to grow at the expense of the L_β phase for the duration of the experiment (15 min; Fig. 7). Translation of the sample by 2 mm to one side of the original exposed site revealed the presence of the L_β phase alone, indicating that loss of temperature control during the experiment was not a problem. This experiment demonstrates clearly that x-radiation can induce damage to the products of which can lower the onset temperature of the L_β-to-L_α transition in the DEPE/water system. A more complete and systematic study of radiation damage to DEPE was not performed nor indeed were the products of radiation damage identified. Suffice it to say that for x-ray sensitive samples, such as DEPE, a suitable exposure strategy that may include intermittent sample exposure must be implemented so as to minimize or obviate the radiation damage problem during SCALTRD measurements.

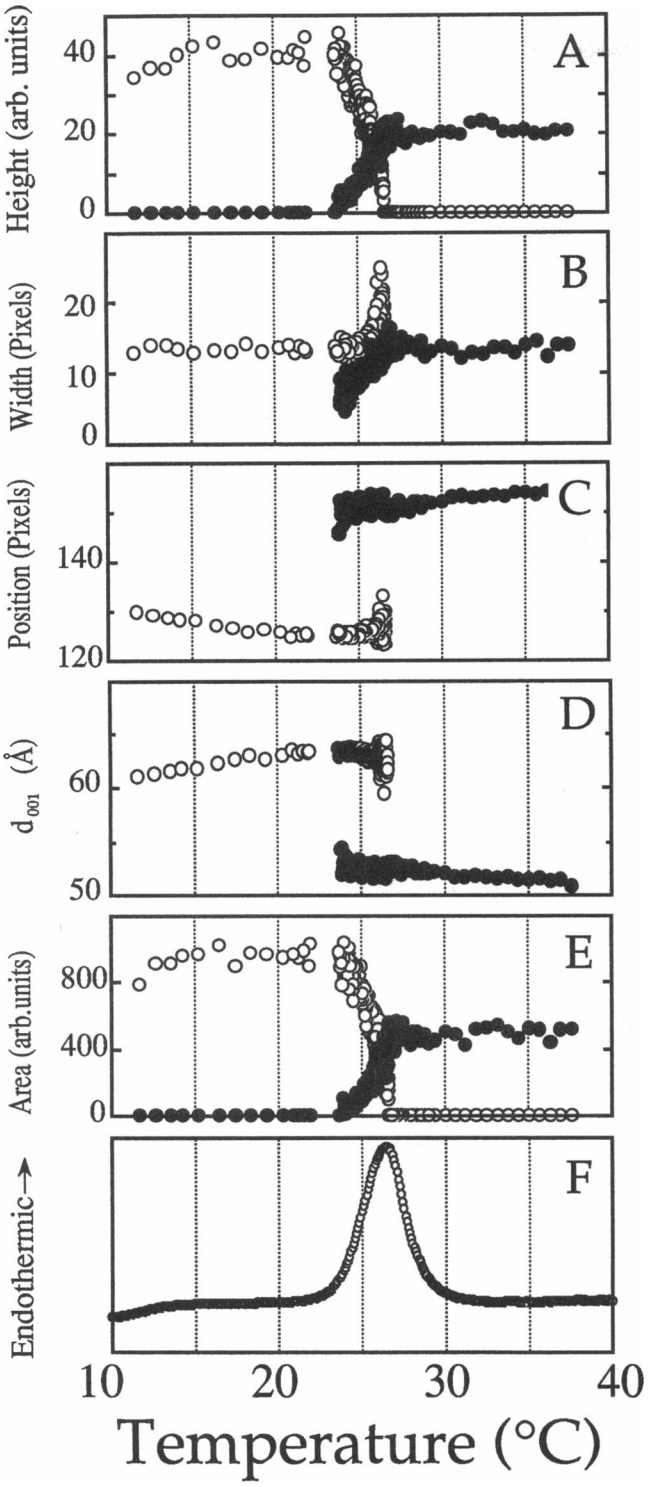

FIGURE 5 Progress of the L_β-to-L_α phase transition in fully hydrated monoelaidin induced by a temperature ramp at 5°C/min during the course of a simultaneous calorimetry and TRXRD. The x-ray diffraction data are shown in *A–E* and the calorimetric thermogram is presented in *F*. The open and closed symbols in *A–E* correspond to the L_β and L_α phases, respectively. The low-angle (001) diffraction peak maximum intensity is shown in *A*, the half-width at half-height in *B*, the radial position of the peak maximum in *C*, the d-spacing of the peak maximum in *D*, and the integrated diffracted intensity or peak area in *E*. *A–E* and *F* each contain ~360 and 300 discrete data points, respectively. The increase in the spread of the data in *B–D* in the coexistence region arises as a result of error in fitting the 001 lamellar diffraction peak of the nascent L_α and decaying L_β phase when either is present in small amounts.

DISCUSSION

Comparison between calorimetry and TRXRD and the nature of the transition

The results obtained using calorimetry and TRXRD in SCALTRD measurements on the L_β-to-L_α transition of fully hydrated monoelaidin are compared in Fig. 8. The data in Fig. 8 *A* demonstrate convincingly the agreement that exists between the two methods when SCALTRD measurements are performed at lower scan rates. As the scan rate increases, so too does the disparity between the two techniques, particularly in regard to transition midpoint and completion temperatures.

To what can we ascribe the origin of the mismatch between calorimetry and TRXRD observed in the SCALTRD measurement made at higher scan rates? There are several possibilities. To begin with, the x-ray beam used is small (0.5 mm diameter) in comparison to the dimension of the sample crucible (5.5 mm diameter). Thus, only a fraction of the sample (~2% by vol) located at the center of the crucible is actually interrogated by TRXRD. In contrast, the calorimeter is responding to the heat of the transition absorbed throughout the bulk of the sample. The second possibility concerns gradients that exist within the sample. Referring to Fig. 1, the sample is heated from the left-hand side by contact with the heating block and base plate. It is also heated from the right-hand side by contact between the open lid and the heating block. Thus, it is likely that sizable thermal gradients exist within the sample at higher heating rates such that the region interrogated by TRXRD will respond in a manner somewhat differently to that of the bulk. The shift to higher completion temperatures at the higher heating rates undoubtedly reflects the fact that the thermocouple sensors are located on the base plate in contact with the heating block and not in the sample. As a result, there is a thermal lag associated with communicating heat between the heater and the bulk of the sample. The excellent agreement between the data obtained by calorimetry and TRXRD at a heating rate of 1°C/min in SCALTRD measurements indicates the need for slow scan rates if structure and thermodynamic data are to be correlated directly.

The following evidence suggests that the L_β-to-L_α phase change in hydrated monoelaidin involves only the L_β and L_α phases during the course of the transition. To begin with, the 001 reflections from the L_β and L_α phases both coexist throughout the transition. Second, within the sensitivity limits of the method, no intermediates were observed during the phase transition. Third, there is no loss of correlation in the lamellar structure of either

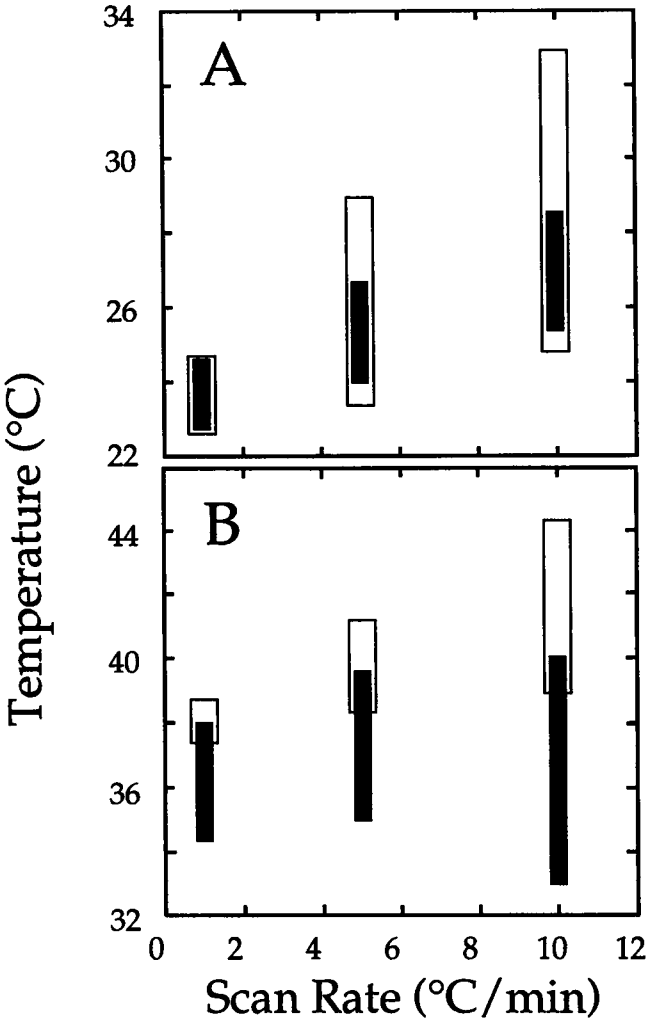

FIGURE 6 Comparison of the L_β-to-L_α phase transition temperature ranges for (*A*) monoelaidin and (*B*) DEPE in excess water determined by simultaneous calorimetry and TRXRD at different heating rates. The transition temperature range for calorimetry and TRXRD are represented by open and filled rectangular boxes, respectively. The bottom and top of each box corresponds, respectively, to the onset and completion temperature of the transition. The calorimetric onset and completion temperatures were determined as the intercept of the low and high temperature baselines with the extrapolated rising and falling edge of the endothermic peak. The diffraction based onset and completion temperatures correspond, respectively, to those temperatures where the first trace of the nascent L_α phase and the last trace of the decaying L_β phase is apparent by visual inspection of the live-time diffraction patterns.

phase during the transition as evidenced by the fact that the shape and width of the 001 reflections of both phases remains essentially constant throughout the transition.

In the following, we set about establishing a means for directly comparing the calorimetric and TRXRD data obtained during SCALTRD. We begin this analysis by noting that the area under the experimentally measured diffraction peak in an I-2θ scan is proportional to the amount of material giving rise to the diffraction peak (Klug and Alexander, 1974). Thus, we can write that the fraction of lipid existing in each phase during the L_β-to-L_α transition is given by

$$\theta_\alpha = \frac{NA_\alpha}{A_\beta + NA_\alpha} \tag{4}$$

and

$$\theta_\beta = \frac{A_\beta}{A_\beta + NA_\alpha} = 1 - \theta_\alpha, \tag{5}$$

where A is the integrated intensity of the 001 reflection, N is a normalization factor corresponding to the ratio of the integrated intensities of the 001 reflection in the pure phase region, and the subscripts α and β refer to the L_α and L_β phases, respectively. From the data in Fig. 5 *E*, it is apparent that the integrated intensities of the 001 reflection in the pure L_β and L_α phases are different. This necessitates the use of a normalization factor in Eqs. 4

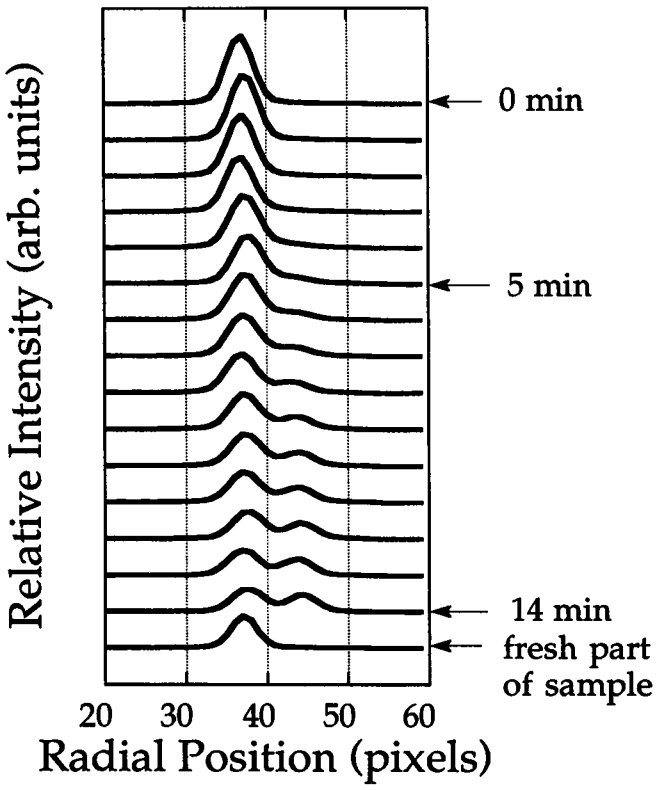

FIGURE 7 X-radiation damage to fully hydrated DEPE at 35.4 ± 0.5°C in the L_β phase. Low-angle 001 diffraction data were recorded on an image plate using a remotely controlled shuttered streak camera under conditions of continuous x-ray exposure. Each plot corresponds to an I-20 scan across the diameter of the diffraction rings from the digitized image plate data. Scans are shown sequentially from top to bottom each corresponding to an exposure of 1-min duration. In the early stages of the experiment, only the L_β phase is present. A second peak corresponding to the L_α phase emerges after ~5 min of exposure and grows continuously at the expense of the L_β phase with continued exposure. The last scan shows the pure L_β phase in a fresh unexposed part of the sample some 2 mm away from the original exposure site. Scans are displaced vertically on the ordinate for clarity.

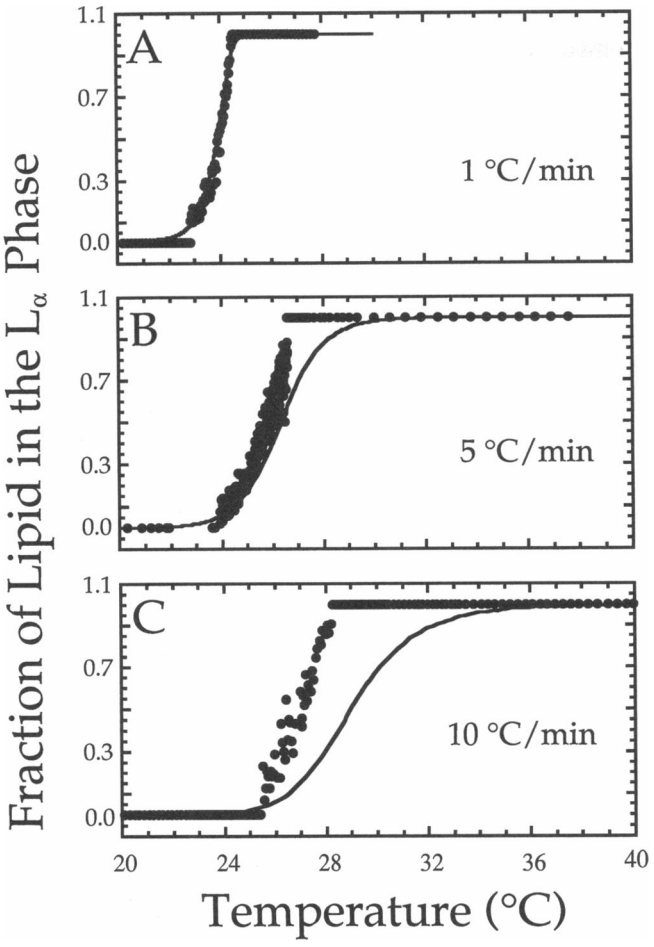

FIGURE 8 Comparison of the integrated calorimetric thermograms (*solid lines*) and the fraction of lipid in the L_α phase determined from TRXRD data (*filled circles*) recorded during simultaneous calorimetry and TRXRD measurements on fully hydrated monoelaidin at different heating rates.

and 5. Such a difference is attributable, in part, to differences in phase density of magnitude, typically 10% (Nagle and Wiener, 1988; Marsh, 1990). The major difference in integrated intensity most likely originates from the disparate structure factors that apply to the 001 reflection in each phase. For Eq. 4 and 5 to hold, it is necessary that the corresponding structure factors remain constant during the transition. In the absence of knowing the structure factor profile for the two phases, the following is presented in support of the requirement for a constant structure factor through the transition. Referring to Fig. 5 *D*, we see that the change in the lamellar repeat distance of either the L_β or L_α phases in the single phase region amounts to ~2 Å. In this same temperature interval, the integrated intensity (area) of the 001 reflection in either phase remains essentially constant (Fig. 5 *E*). This suggests, therefore, that in both cases the corresponding structure factors are close to their maximum values and are relatively insensitive to changes in lattice parameter. By comparison with other hydrated lipid systems where the structure factor profile is known, a 2-Å change in d-spacing gives rise to a 1, 20, and 100% change in structure factor at the maximum, half-maximum, and near-zero structure factor values, respectively (Kim et al., 1987; Hogan, 1989; Caffrey et al., 1991*b*). Because the reciprocal spacings of the 001 reflections do not change significantly [$\geq(0.5\ \text{Å})^{-1}$, corresponding to a d-spacing change of ≤ 0.5 Å] during the course of the transition (see Fig. 5 *D*), we consider that use of Eqs. 4 and 5 in the analysis is appropriate. The value of N used in the analysis that follows is $[(960 \pm 60)/(470 \pm 90)] = 2.0 \pm 0.4$ (see Fig. 5 *E*).

After this analysis, the progress curve for the L_β-to-L_α transition observed by TRXRD is shown in Fig. 8, where θ_α (*filled circles*) is plotted as a function of temperature through the transition. The integrated calorimetric thermograms (*solid lines*) recorded simultaneously with the TRXRD are included to facilitate comparison. The agreement between the two methods is demonstrated convincingly at the slowest heating rate.

Radiation damage

The potential for radiation-induced chemical breakdown of a sample during SCALTRD measurements is high because of the lengthy exposures to an intense x-ray beam during the course of the temperature scan. This means that the local accumulated radiation dose can be high for a stationary sample under conditions of continuous exposure. Furthermore, the effect can be sample specific as evidenced in this study. Thus, although DEPE proved x-ray sensitive under conditions of measurement, monoelaidin did not.

Our original SCALTRD measurements on the L_β-to-L_α transition of fully hydrated DEPE gave confusing results. Consistently, at all heating rates used, the transition began and was completed at lower temperatures when observed by TRXRD. Temperature gradients in the sample could not explain this result because a lower scan rate should give a better agreement between calorimetry and TRXRD and should reduce the transition range determined by both techniques.

We speculated that radiation damage was the cause of the discrepancy between the two methods and of the dramatic lowering of the onset temperature of the transition observed by TRXRD. A TRXRD measurement on hydrated DEPE incubated 2.2°C below the L_β-to-L_α transition temperature demonstrated the appearance of the L_α phase in an L_β background on continuous x-ray exposure (Fig. 7). The L_α phase grew at the expense of the L_β phase throughout the experiment. This result showed convincingly that x-ray exposures on the time scale of the current SCALTRD experiments are sufficient to induce radiation damage and to alter the mesophase properties of the lipid. Furthermore, although TRXRD is performed on and is responding to the very same volume that is undergoing radiation damage, the calorimetric

measurement is responding to >98% of the sample volume that has not succumbed to damage and is still fresh. It is not unreasonable, therefore, to expect a different behavior monitored by TRXRD and calorimetry in SCALTRD measurements where radiation damage effects are significant.

The problem of radiation damage can be minimized by moving the sample continuously in the x-ray beam and/or by intermittent exposure to the x-ray beam. The object in both cases is to ensure that any one part of the sample is not exposed to x-rays for a period long enough to induce damage. Alternatively, with an x-ray source of large divergence, the optical arrangement can be such as to focus x-rays not on the sample but on the detector. This has the effect of distributing the incident flux over a larger area and of reducing the accumulated dose at any one location in the sample. Such was the arrangement at NSLS. Indeed, with this configuration, the transition range measured by TRXRD was within that observed by calorimetry at a scan rate of 5°C/min for DEPE/water (data not shown). However, we must note that a direct comparison between NSLS and CHESS is not appropriate because of the differences in overall flux and x-ray energies used. Flux was lower at NSLS and the energies used were 8.0 and 13.8 keV at CHESS and NSLS, respectively.

These results serve to highlight the potential problems associated with radiation damage during SCALTRD measurements and the need to investigate the magnitude of the effect on a per sample basis. The issue of synchrotron x-radiation damage of lipids is an ongoing concern in this laboratory (Caffrey, 1984; Cheng and Caffrey, 1991, 1992; Cheng and Caffrey, manuscript in preparation).

CONCLUSIONS

Simultaneous calorimetry and TRXRD has been carried out successfully on a single hydrated lipid sample. This "methods in combination" approach provides for a direct correlation of thermodynamic and structural information free of artifacts that can arise as a result of differences in sample thermal history, preparation, and source when the measurements are performed separately. At low scan rates, the results obtained by calorimetry and by TRXRD agree well in SCALTRD measurements. At higher scan rates, a disparity arises as a result of differences in the sample volumes interrogated by the two methods and the existence of thermal gradients in the sample. Radiation damage was found to be an important issue for SCALTRD measurements as a result of fact that the exposure times used are long, and a very intense x-ray source is needed to make the TRXRD measurements. The damaging effect appears to be sample specific and must be evaluated on an individual case basis. Despite the problems, SCALTRD is a powerful method for collecting structural and thermal data on systems where separate measurements under identical conditions are impractical.

We thank the entire CHESS (National Science Foundation grant DMR 12822), MacCHESS (National Institutes of Health grant RR-014646), and NSLS (Department of Energy grant KP04-01 and -BO43) staff for their invaluable help and support. We also thank S.-T. Lin for revising the least-square fitting program used in data analysis and J. Briggs, A.-C. Cheng, J. Hogan, A. Mencke, J. Wang, and T. Zhu for critical comments on this manuscript and for valuable discussions.

This work was supported by a grant from the National Institutes of Health (DK-36849).

Received for publication 30 January 1992 and in final form 10 April 1992.

REFERENCES

Caffrey, M. 1984. X-radiation damage of hydrated lecithin membranes detected by real-time x-ray diffraction using wiggler-enhanced synchrotron radiation as the ionizing radiation source. *Nuclear Instruments and Methods in Physics Research.* 222:329–338.

Caffrey, M. 1985. Kinetics and mechanism of the lamellar gel/lamellar liquid crystal and lamellar/inverted hexagonal phase transition in phosphatidylethanolamine: a real-time x-ray diffraction study using synchrotron radiation. *Biochemistry.* 24:4826–4844.

Caffrey, M. 1987. Kinetics and mechanism of transitions involving the lamellar, cubic, inverted hexagonal, and fluid isotropic phases of hydrated monoacylglycerides monitored by time-resolved x-ray diffraction. *Biochemistry.* 26:6349–6363.

Caffrey, M. 1989. The study of lipid phase transition kinetics by time-resolved x-ray diffraction. *Annu. Rev. Biophys. Biophys. Chem.* 18:159–186.

Caffrey, M., J. Hogan, and A. Mencke. 1991*a*. Kinetics of the barotropic ripple ($P_{\beta'}$)/lamellar liquid crystal (L_α) phase transition in fully hydrated dimyristoylphosphatidylcholine (DMPC) monitored by time-resolved x-ray diffraction. *Biophys. J.* 60:456–466.

Caffrey, M., J. Hogan, and A. S. Rudolph. 1991*b*. Diacetylenic lipid microstructures: Structural characterization by x-ray diffraction and comparison with the saturated phosphatidylcholine analogue. *Biochemistry.* 30:2134–2146.

Caffrey, M., R. L. Magin, B. Hummel, and J. Zhang. 1990. Kinetics of the lamellar and hexagonal phase transitions in phosphatidylethanolamine: time-resolved x-ray diffraction study using a microwave-induced temperature jump. *Biophys. J.* 58:21–29.

Cheng, A., and M. Caffrey. 1991. X-radiation damage of aqueous phospholipid dispersions monitored by x-ray diffraction. *Biophys. J.* 59:634*a*. (Abstr.)

Cheng, A., and M. Caffrey. 1992. Observation of an x-radiation damage-induced H_{II} phase in fully hydrated DHPE. *Biophys. J.* 61:1777.

Finegold, L., S. J. Melnick, and M. A. Singer. 1985. The thermal properties of dilaurylphosphotidylethanolamine liposomes are affected by lipid source and preparation. *Chem. Phys. Lipids.* 38:387–390.

Garti, N., and K. Sato, editors. 1988. Crystallization and Polymorphism of Fats and Fatty acids. Marcel Dekker, Inc., New York. 450 pp.

Hogan, J. L. 1989. The polymorphism of headgroup methylated phosphatidylethanolamines. Ph.D. thesis. The University of Southampton, England. 279 pp.

Kellens, M., W. Meeussen, R. Gehrke, and H. Reynaers. 1991*a*. Synchrotron radiation investigations of the polymorphic transitions of saturated monoacid triglycerides. Part 1: Tripalmitin and tristearin. *Chem. Phys. Lipids.* 58:131–144.

Kellens, M., W. Meeussen, A. Hammersley, and H. Reynaers. 1991*b*. Synchrotron radiation investigations of the polymorphic transitions in saturated monoacid triglycerides. Part 2: Polymorphism study of a 50:50 mixture of tripalmitin and tristearin during crystallization and melting. *Chem. Phys. Lipids.* 58:145–158.

Kim, J. T., J. Mattai, and G. G. Shipley. 1987. Gel phase polymorphism in ether-linked dihexadecylphosphatidylcholine bilayers. *Biochemistry.* 26:6592–6598.

Klug, H. P., and L. E. Alexander. 1974. X-Ray Diffraction Procedures: For Polycrystalline and Amorphous Materials. 2nd ed. John Wiley & Sons, Inc., New York. 966 pp.

Luzzati, V. 1968. X-ray diffraction studies of lipid-water systems. *In* Biological Membranes. Vol. 1. D. Chapman, editor. Academic Press, New York. 71–123.

Macgillavry, C. H., and G. D. Rieck, editors. International Tables for X-Ray Crystallography. 1962. Vol. III. The Kynoch Press, Birmingham, England. 362 pp.

Marsh, D. 1990. Handbook of Lipid Bilayers. CRC Press, Boca Raton, FL. 387 pp.

Martin, J. 1953. Preparation of saturated and unsaturated symmetrical monoglycerides. *J. Am. Chem. Soc.* 75:5482–5486.

McElhaney, R. N. 1986. Differential scanning calorimetric studies of lipid-protein interactions in model membrane systems. *Biochim. Biophys. Acta.* 864:361–421.

Mencke, A. P., and M. Caffrey. 1991. Kinetics and mechanism of the pressure-induced lamellar order/disorder transition in phosphatidylethanolamine: a time-resolved x-ray diffraction study. *Biochemistry.* 30:2453–2463.

Nagle, J. F., and M. C. Wiener. 1988. Structure of fully hydrated bilayer dispersions. *Biochim. Biophys. Acta.* 942:1–10.

Russell T. P., and J. T. Koberstein. 1985. Simultaneous differential scanning calorimetry and small-angle x-ray scattering. *J. Polym. Sci. Polym. Phys.* 23:1109–1115.

Seddon, J. M., K. Harlos, and D. Marsh. 1983. Metastability and polymorphism in the gel and fluid bilayer phases of dilauroylphosphatidylethanolamine: two crystalline forms in excess water. *J. Biol. Chem.* 258:3850–3854.

Slater, J. L., C. H. Huang, R. G. Adams, and I. W. Levin. 1989. Polymorphic phase behavior of lysophosphatidylethanolamine dispersions. A thermodynamic and spectroscopic characterization. *Biophys. J.* 56:243–252.

Small, D. M. 1986. Handbook of Lipid Research. The Physical Chemistry of Lipids from Alkanes to Phospholipids. Vol. 4. Plenum Publishing Corp., New York. 672 pp.

Ungar, G., and J. L. Feijoo. 1990. Simultaneous x-ray diffraction and differential scanning calorimetry (XDDSC) in studies of molecular and liquid crystals. *Mol. Cryst. Liq. Cryst.* 180B:281–291.